Nanomed Res J 9(3):264-273, Summer 2024

RESEARCH ARTICLE

Magnetic loaded compritol ATO based lipid carriers as a targeted anti-cancer drug delivery system

Elham Rostami *

Department of Chemistry, Faculty of Science, Shahid Chamran University of Ahvaz, Ahvaz, Iran

ARTICLE INFO

Article History:
Received 17 May 2024
Accepted 23 June 2024
Published 01 Aug 2024

Keywords:
Magnetic Lipid Nanoparticle
Target drug delivery
Stearic Acid
Compritol ATO 888

ABSTRACT

In this study, we prepared Epirubicin-loaded magnetic solid lipid nanoparticles for intravenous drug dosing. Magnetic lipid carriers were fabricated using a hot microemulsion approach using stearic acid and Compritol ATO 888 as a core of particles. Prepared nanoparticles are characterized using transtition electon microscopy, photon correlation spectroscopy, Fourier transforms infrared spectroscopy, and vibrating sample magnetometer. The size of nanoparticles was about 130 nm after drug loading. Also, entrapment efficiency, drug loading, in vitro drug release, and release kinetic were investigated in detail. In vitro cell cytotoxicity and biocompatibility of particles evaluated by MCF-7 cell lines. The entrapment efficiency of 86±4.5% and 51.7±3.5% were obtained for solid lipid and magnetic solid lipid nanoparticles respectively. Size investigation showed that prepared NPs have an increase in particle size with magnetic loading. In vitro cytotoxicity of the formulations on the MCF-7 cell line demonstrated the greater toxicity of drug-loaded nanoparticles compared to the free drug. This study proved the efficiency of lipid-based carriers in drug dosing and targeting. These studies showed that the Magnetic Lipid Nanoparticle (mSLN) has a very remarkable anticancer effect on the MCF-7 cell line in comparison with pure drug.

How to cite this article
Rostami E. Magnetic loaded compritol ATO based lipid carriers as a targeted anti-cancer drug delivery system. Nanomed Res J, 2024; 9(3): 264-273. DOI: 10.22034/nmrj.2024.03.004

INTRODUCTION

Cytotoxic drugs continue to be the primary type of chemotherapy used in cancer treatment. This diverse group of therapeutic agents primarily targets rapidly growing and dividing cells, leading to the destruction of cancerous cells [1]. These drugs are usually delivered intravenously through bolus or infusion, predominantly in the form of free drug solutions. Even with the extensive history of anticancer drugs and the creation of various new multi-drug combinations for enhanced clinical outcomes, treatment failures are still commonly observed [2].

Since the beginning of the 1990s, solid lipid nanoparticles (SLN) have been recognized as a promising alternative to conventional drug delivery systems [3, 4]. In comparison to conventional carriers, SLNs provide a unique blend of benefits associated with both polymeric nanoparticles (NPs) and emulsions, including low toxicity, excellent biocompatibility, and targeted delivery to the brain [5]. These nanoparticles have been administered through various routes, including parenteral, oral, dermal, ocular, pulmonary, and rectal applications [6-8]. Furthermore, their biocompatibility supports their use in intravenous drug delivery systems [9, 10].

Iron oxide nanoparticles (NPs) exhibiting superparamagnetic properties are frequently employed as magnetically responsive agents that can be directed within the body by an external magnetic field [11]. Although magnetic nanoparticles (mNPs) are physiologically inert, following intravenous administration, they can become adsorbed by plasma proteins or may be removed from the bloodstream as part of the initial clearance process conducted by the reticuloendothelial system [12]. To enhance their circulation time in

* Corresponding Author Email: *e.rostami@scu.ac.ir*
Elhamrostami74@gmail.com

the bloodstream, surface modification of mNPs through the application of hydrophilic polymers and proteins can reduce plasma component adsorption [13, 14]. Furthermore, iron oxide NPs have been utilized in the realm of magnetic drug targeting [15, 16].

In recent years, Magnetic Solid Lipid Nanoparticles (mSLNs) have emerged as a novel drug delivery system with significant potential in cancer therapy [17, 18]. The incorporation of magnetic nanoparticles (mNPs) allows SLNs to be directed to tumor sites via blood circulation using a magnetic field. As a result, the toxicity and dosage of chemotherapy drugs are reduced, while the reliability, effectiveness, and patient adherence to these treatments are notably enhanced [19]. However, the effect of using different lipids on drug release and its toxicity to achieve a commercial formulation is still the subject of many studies. The use of lipids with different and constant chains can have a more appropriate effect on improving cytotoxicity, which has been studied in fewer studies.

The present study discussed the preparation and optimization of Epirubicin (EPI) loaded SLNs and mSLNs and evaluated their effectiveness for cellular localization and cytotoxicity. Magnetic-loaded SLNs encapsulating EPI were prepared and characterized in size, uniformity, and magnetic properties. Moreover, studies of kinetics EPI release were explored using first-order, Higuchi, zero-order, and Krosmeyer-Peppas models. The formulations were subsequently evaluated for in vitro cellular uptake and cytotoxic effects on MCF-7 cells, and results were compared with those of the free drug. The primary aim of this study is to develop and utilize a novel nano-carrier for EPI.

MATERIALS AND METHODS

Materials

Epirubicin, with a purity of 99.8%, was sourced from Yuanjian Pharmaceutical Technology Development Co. in China. Fe(II) chloride tetrahydrate (99%), Fe(III) chloride hexahydrate (97%), and stearic acid were procured from Merck, located in Darmstadt, Germany. Compritol ATO 888 (glycerol dibehenate) was generously provided by Gattefossé in the UK. 3-(4,5-dimethylthiazol-2-yl)-2,5-diphenyltetrazolium bromide (MTT) was procured from Sigma Aldrich (St. Louis, MO, USA). MCF-7 (Michigan Cancer Foundation-7) cells were acquired from the Pasteur Institute (National Cell Bank of Iran). All other reagents were of the highest purity and sourced from commercial suppliers.

Synthesis of Fe_3O_4 magnetic NPs and mSLNs preparation

Iron oxide mNPs were synthesized by combining $FeCl_3.5H_2O$ and $FeCl_2.4H_2O$ in a 2:1 molar ratio in 20 mL of distilled deionized water at a temperature of 60 ◦C under a nitrogen atmosphere, with stirring maintained at 250 rpm for 15 minutes. Subsequently, 100 mL of 8 M NH_4OH was introduced into the solution, causing an immediate color change from yellow to black. The mixture was then stirred at 400 rpm for an additional 10 minutes [20]. The resulting mNPs were rinsed three times with 5% NH_4OH.

In general, microemulsions were formulated using oil/water (O/W) systems with surfactants and co-surfactants. The oil droplets were stabilized by a layer of adsorbed stabilizer at the interface between the two liquids. Solid Lipid Nanoparticles (SLNs) were produced through an O/W microemulsion technique, utilizing Compritol ATO 888 and stearic acid (SA) as the lipid core. The preparation parameters were fine-tuned in accordance with Table 1. An aqueous solution was made with 10 mL of distilled deionized water (dd-H2O) containing Tween 80, which was heated to 75 ºC. A mixture of 30 mg of Compritol ATO 888 and 20 mg of SA was melted at a temperature 10 ºC above the lipid's melting point (75 ºC), after which a specific amount of EPI and mNPs was incorporated into the oily phase. The resultant microemulsion was stirred for 30 minutes at 1000 rpm. Following this, the mixture was sonicated for 2 minutes using a probe sonicator operating at 60 W, while maintaining a constant temperature of 75 ºC. The mSLNs were produced by introducing the hot emulsion into chilled water (at a temperature of 2-5 ºC) in a ratio of 1:5 (addition rate: 2 mL/min, using a 25-gauge syringe needle, and a stirring speed of 750 rpm). Nanosized mSLNs were produced through ultra-sonication employing a probe sonicator (60 W) for 2 minutes while kept in an ice bath. To eliminate the surfactant and any unentrapped EPI, the mSLNs were dialyzed using a cellulose acetate dialysis bag with a molecular weight cutoff of 12 kDa for 30 minutes in deionized water. The resulting dialyzed solution was utilized for calculating drug loading (DL) and entrapment efficiency (EE). Finally, the sample was freeze-dried using a freeze dryer for further assessments and experiments.

Determination of Encapsulation efficiency

EE (%) and DL (%) were determined using the methodology outlined earlier. The amount of EPI incorporated into mSLNs was quantified using UV-VIS spectroscopy. A UV-VIS calibration curve for EPI was created by measuring its absorbance at 309 nm, while spectrophotometric analysis was performed at 302 nm using a Shimadzu spectrophotometer from Japan. The drug EE within the NPs was calculated according to equations (1) and (2): [21]

$$EE\ (\%)=\left(\frac{W_a-W_s}{W_a}\right)\times 100 \quad (1)$$

$$DL\ (\%)=\left(\frac{W_a-W_s}{W_a-W_s+W_L}\right)\times 100 \quad (2)$$

where W_a, W_s, and W_L represent the added amount of EPI for the NPs preparation, the mass of EPI in the dialyzed media, and the mass of used lipids in the mSLNs preparation, respectively.

Characterization of synthesized magnetic nanoparticles

The particle size and polydispersity index (PDI) of the nanoparticles (NPs) were determined using Photon Correlation Spectroscopy (PCS) with a Malvern Zetasizer ZS (Malvern, UK). The dried powder samples were suspended in ultra-pure water and subjected to mild sonication prior to measurement. The average diameter and PDI of the resulting homogeneous suspension were then evaluated. Spectra for Fourier-transform infrared spectroscopy (FTIR) were obtained for EPI, SA, Compritol ATO 888, mNPs, and mSLNs using an infrared spectrophotometer (Perkin Elmer Spectrum BX, USA). The samples were blended with dry powdered potassium bromide and subjected to high-pressure compression. The resulting transparent disks were analyzed across a wavelength range of 4,000 to 400 cm-1. The magnetization of the synthesized nanoparticles was assessed using a vibrating sample magnetometer (VSM) (HH-15, Nanjing University Instrument Plant, China) at room temperature.

In vitro release and kinetics evaluation

The *in vitro* release of nanoparticles was assessed using the dialysis technique involving a Franz diffusion cell. Specifically, 10 mg of freeze-dried nanoparticles, suspended in 0.2 M phosphate-buffered saline (PBS) at pH 7.4, was positioned in the donor compartment, while 50 mL of PBS was placed in the receptor compartment. The setup was incubated at 37°C with magnetic stirring at 400 rpm. At predetermined intervals, 500 µL of the medium was withdrawn and replaced with an equal volume of fresh PBS. For the analysis of the drug content, the collected samples were acidified using 5% perchloric acid to determine the total concentration of EPI [22]. In this work, dissolution model approaches are utilized to evaluate the release profiles of EPI from the carrier [23, 24]. These model-dependent methods involve fitting the release data to several equations: zero-order (Eq. 2), first-order (Eq. 3), Higuchi matrix (Eq. 4), Peppas–Korsmeyer (Eq. 5), and Hixson–Crowell (Eq. 6).Zero-order (Eq. 3) data are plotted as cumulative percentage drug released *vs* time. Where C is the concentration of the drug in the t and K_0 is the zero-order rate constant.

$$C = K_0 t \quad (2)$$

The first order (Eq. 4) is obtained by plotting log cumulative release vs time.

$$\text{Log } C = \text{Log } C_0 - Kt/2.303 \quad (3)$$

As per Higuchi's (Eq. 4) data is plotted as a cumulative percentage of drug released *vs* the square root of the time.

$$Q = Kt^{1/2} \quad (4)$$

The drug release mechanism is assessed by graphing the percentage of drug released against the logarithm of time, following the Korsmeyer-Peppas equation.

$$M_t/M\infty = Kt^n \quad (5)$$

Where $M_t/M\infty$ is the fractional solute release, t is the release time.

Cytotoxicity studies

A MTT test was used to assess the viability of the cells following the optimization of both NP formulations. A density of 1.5 104 cells/well was plated in 96-well plates (NalgenNunc International, Ochester, NY) for 24 h to ensure sufficient adhesion. A 96-well plate was incubated for 24 h with three different concentrations of mSLNs and

EPI. Incubation was completed by washing the cells with PBS, followed by adding MTT dye solution (10% in phosphate buffer, pH 7.4). Incubation was completed by measuring the optical density of each well via a microplate reader at 540 nm.

(Bio-Tek, ELX 800, USA). A 100% absorbance was set for the untreated culture. As part of the control cytotoxicity experiments, the biocompatibility of drug-free mSLNs at various concentrations was assessed against MCF-7 using the same procedure described above.

RESULTS AND DISCUSSION

Nanoparticles characterization

Iron oxide magnetic nanoparticles (mNPs) were synthesized through the chemical co-precipitation of ferric and ferrous salts in an alkaline environment. Before magnetic loading to lipid media, the SLNs preparation parameters are optimized (Table 1). In continue magnetic particles (2.5 mg) were probe sonicated, and to prevent aggregation of mNPs, lipids were used as a dispersing agent and coated the mNPs and the drug. Table 1 shown the particle size and PDI value of fabricated SLNs.

The size of mSLNs was inspected utilizing TEM pictures. Fig. 1 (a) shows the circular shape of mSLNs with a breadth of around 107 nm before drug loading and Fig 1(b) shows mSLNs after drug loading around 130 nm. The TEM image showed a spherical-shaped of NPs. The size of mSLN shows about 131 nm in the histogram, and the poly disparity index of mSLN was about 0.247 (Fig.3). All the data confirmed each other.

The primary objective in the preparation of nanoparticles is to achieve full loading of the drug into the carrier, making this investigation extremely significant [25]. To accomplish this aim, the FT-IR spectrum of the pure drug, lipids, SLNs, mSLNs, and Compritol ATO 888 was recorded, as illustrated in Fig. 2.

Fig.2 (a) shows that the FTIR scan of comparator 888 ATO shows a large vibrational

Table 1. The obtained mSLNs in different condition for optimizing the size, PDI and EE%

Formulation	Compritol (mg)	SA (mg)	Tween 80 (ml) (mg)	Hot: Cold Drug (min)	emulsion	mNPs Probe Sonic (hot) (nm)	Size	PDI
F1	50	30	20	5 : 50	---	--- 2	358	0.962
F2	50	30	20	5 : 50	---	--- 2.5	389	0.668
F3	50	30	10	5 : 50	---	--- 3	278	0.920
F4	40	25	10	5 : 50	---	--- 3	314	0.692
F5	30	20	10	10 : 50	---	--- 3	331	0.772
F6	30	20	10	10 : 50	2.5	--- 3 and 3 (cold suspension)	130	0.247
F7	30	20	10	10 : 50	2.5	--- 3 and 3 (cold suspension)	252	0.341

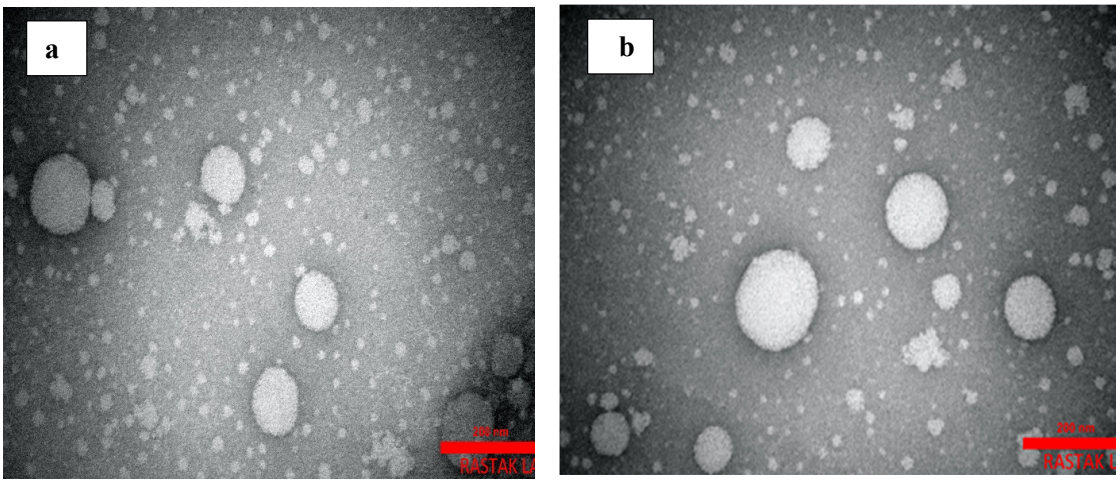

Fig. 1. TEM images of mSLNs (a) before drug loading (b) after drug loading

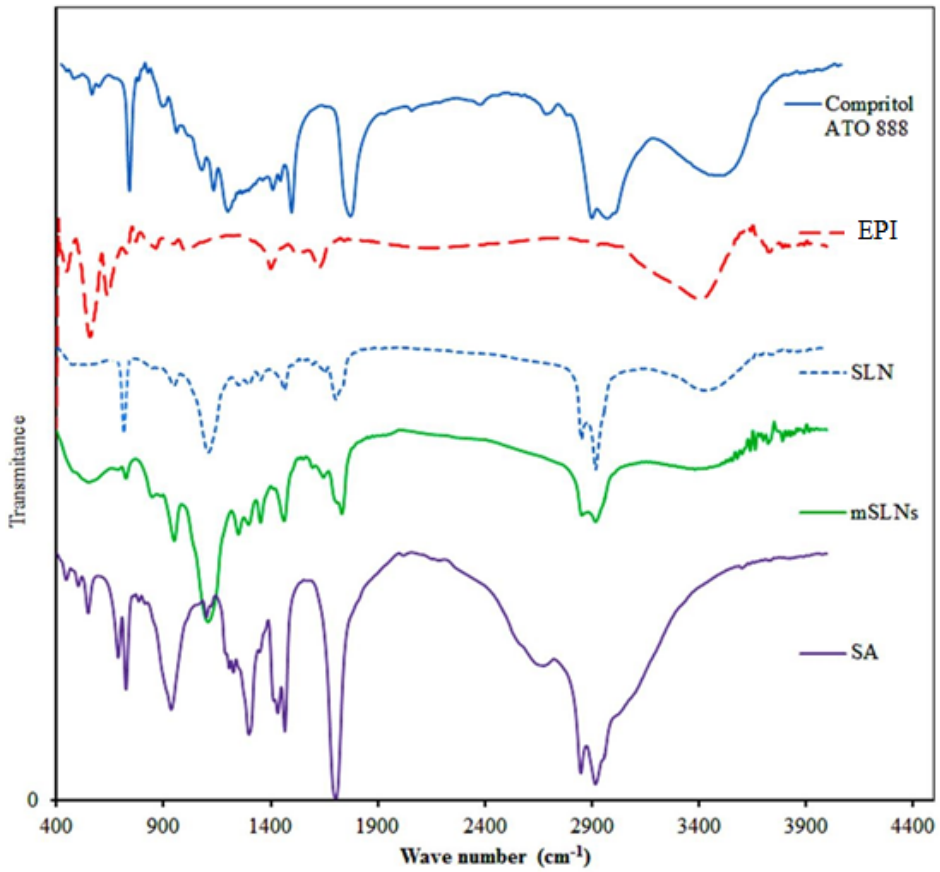

Fig. 2. The FT-IR spectra of samples including(a) Compritol ATO 888, (b) EPI, (c) SLN, (d) mSLNs and (e) SA from 400 to 4000 cm^{-1}

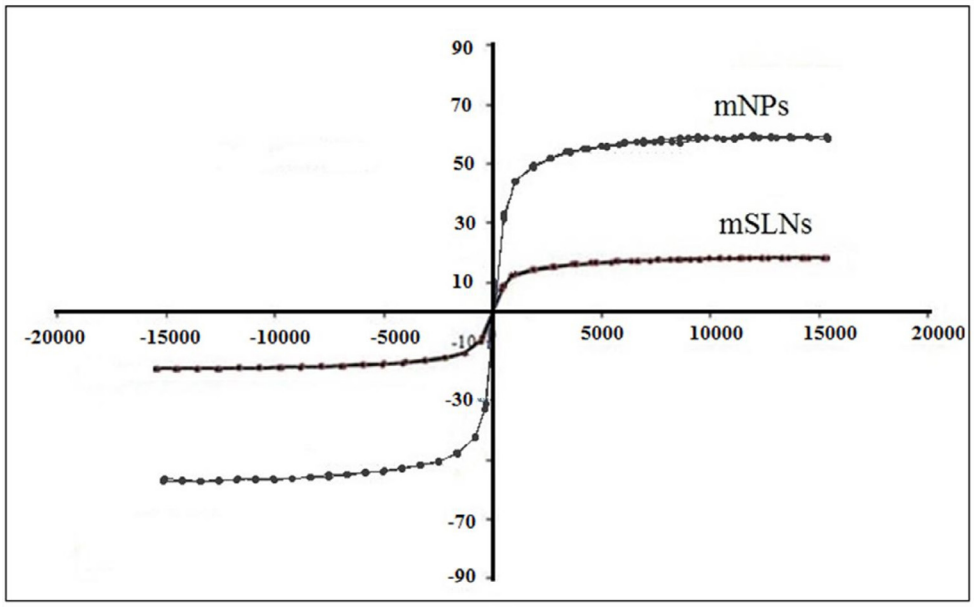

Fig. 3. The VSM spectrum of pure mNPs and mSLN

band caused by the stretching of the -OH groups between 3100 and 3450 cm^{-1}. Between 700 and 1450 cm^{-1}, several vibrational bands appeared, indicating the presence of long triglyceride chains with methylene groups[16-17]. FTIR analysis of Epirubicin shows it contributes to both C=C and C=O stretching modes, while broad peaks at 3435 cm^{-1} correspond to the O–H stretching vibration of water. Specifically, the signals at 1276 cm^{-1} and 1210 cm^{-1} are derived from the enol function (C–O) [25]. The C=O absorption peak was at 1735 cm^{-1}, and C-H stretching absorption bands were at 2847 and 2914 cm. An apparent peak at 1175 cm^{-1} is a characteristic feature of the C-H bending vibration. Based on these observations, it appears that SLNs attach to iron oxide nanoparticles, as indicated by the presence of extra bands at 2912 cm−1 [19].

A diagram showing mSLNs' magnetic properties is shown in Figure 3. The magnetization curve confirmed that MNP's remanence, coercive force, and magnetic hysteresis loop were zero. This indicates that the MNPs possess superparamagnetic behavior. Magnets with a size of less than 10 nanometers experience this phenomenon [26]. According to this result MNPs in SLNs are monodisperse. Magnetic targeted carriers need to be superparamagnetically responsive (i.e. not retain any magnetism despite having been applied with a magnetic field). A saturated magnetization for mSLNs is 14.7 emu/g.

In vitro drug release study

As shown in Fig. 4, the cumulative percentage release profile of EPI under estandarad conditions is expolred *in vitro*. In the first hour following release, initial burst releases were prominent for formulations. Drugs that are encapsulated near the surface of NPs may release an initial burst of drug due to their adhesive properties. In both formulations, drug molecules permeate the lipid core matrix and subsequently leave the dissolution medium, leading to a delayed release [5]. The presence of mNPs on the SLNs causes the difference in the release profile of SLNs.

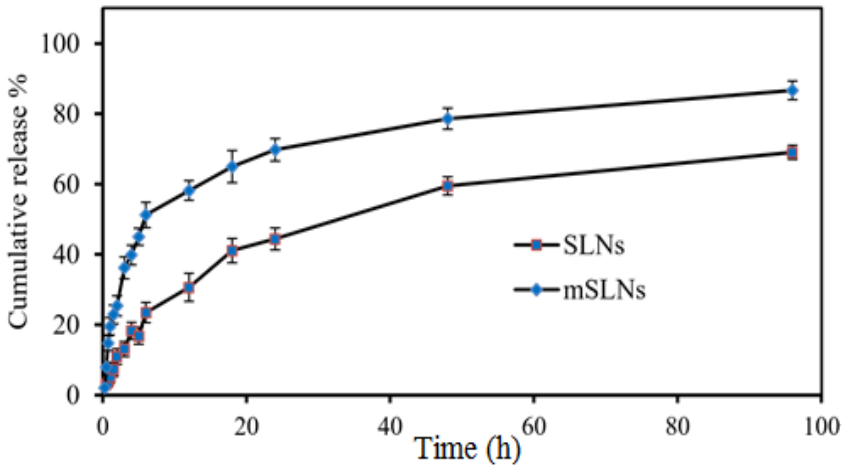

Fig. 4. EPI release of NPs (PBS: pH 7.4, 0.1 M), Error bars (n = 3)

Table 2. The R^2 and K values from *in vitro* release kinetics

Formulas		Zero order	First order	Higuchi model
SLNs	K	0.0067	0.039	8.76
	R2	0.79	0.59	0.99
MSLNs	K	0.008	0.034	11.1
	R^2	0.72	0.54	0.95

K: $\mu g ml^{-1} h^{-1/2}$

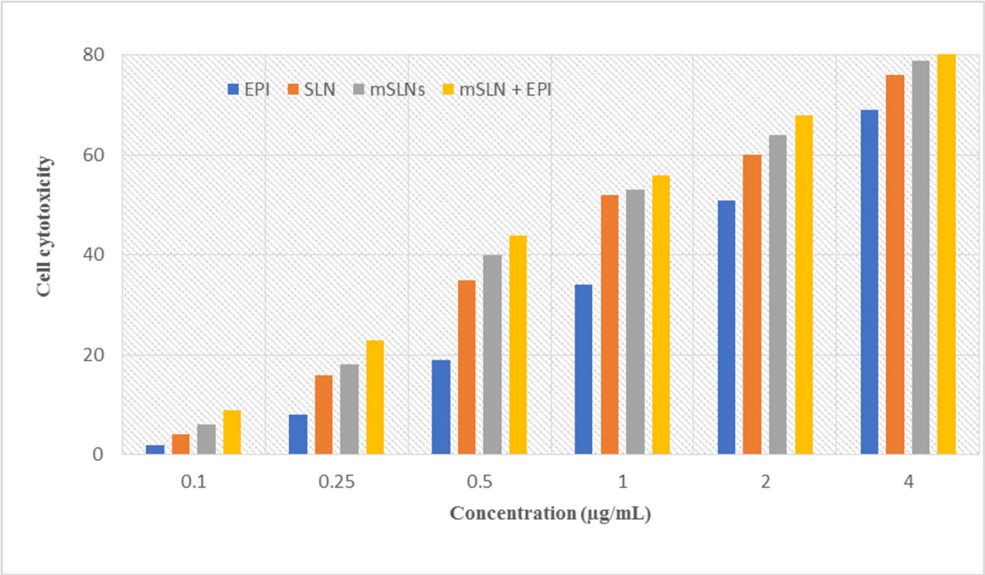

Fig. 4. *In vitro* cytotoxicity of EPI, mSLNs and drug loaded mSLNs (mSLNs + EPI) with different concentration against MCF-7 breast cancer line

The values of R^2 and the dissolution rate constant (K) for the release data of both formulations were obtained by employing the curve fitting technique applied across different kinetic models, which are presented in Table 2. Concerning the release profiles of all formulations, the EPI release adhered to the Higuchi equation more closely, demonstrating higher effectiveness than zero-order kinetics. The Higuchi model serves as an appropriate mechanism for the release of therapeutic agents, characterized by drug diffusion in one dimension, minimal carrier swelling and dissolution, consistent drug molecular size with fixed drug diffusivity, and optimal sink conditions in the release medium for poorly soluble drugs incorporated in nanocarriers with uniform particle size and matrix structure [5]. The release behavior from solid lipid nanoparticles (SLNs) adheres to the Higuchi model due to their shape and structure, as is typical in conventional formulations. Additionally, the release exponent "n" as per the Korsmeyer–Peppas model was also calculated, yielding a value of 0.

In vitro cytotoxicity

Cytotoxicity of epirubicin has been considered in many studies [27]. Releasing EPI from nanoparticles, its cytotoxic activity was evaluated by MTT assay on the MCF-7 cell line after 24 hr exposure to various concentrations of EPI. The dose-effect curves were generated and drug sensitivity to free EPI, mSLNs, and drug-loaded mSLNs was expressed as a drug concentration that caused 50% growth inhibition (IC50). The results indicated that mSLNs have any cytotoxicity effect on cell lines within the measured concentrations as shown in Figure 4. Drug loaded mSLNs had different toxicity.

The biocompatibility of magnetic nanoparticles was important for *iv* drug dosing. Jain et al. were reported any long-term changes in the liver enzyme levels or induce oxidative stress [28-29]. Pang et al. explored the incorporation of MNPs into SLNs for controlled drug release. Their study involved coating MNPs with oleic acid and then loading them into SLNs. In addition to ibuprofen, which has well-established pharmacological properties, mSLNs will also incorporate other drugs. The researchers observed 80% encapsulation efficiency, and magnetic hyperthermia facilitated controlled releases from the nanoformulation when combined with the encapsulated MNPs. SLNs loaded with magnetite are viable alternative delivery systems for drugs, they concluded [30].

The emulsification-diffusion method has also been used by Oliveira and colleagues to create mSLNs that were encapsulated with PTX. Data revealed that magnetic hyperthermia increased the in vitro drug release rate, encapsulation efficiency, and encapsulation efficiency by 67%. According to the researchers, the lipid layer plays a crucial role

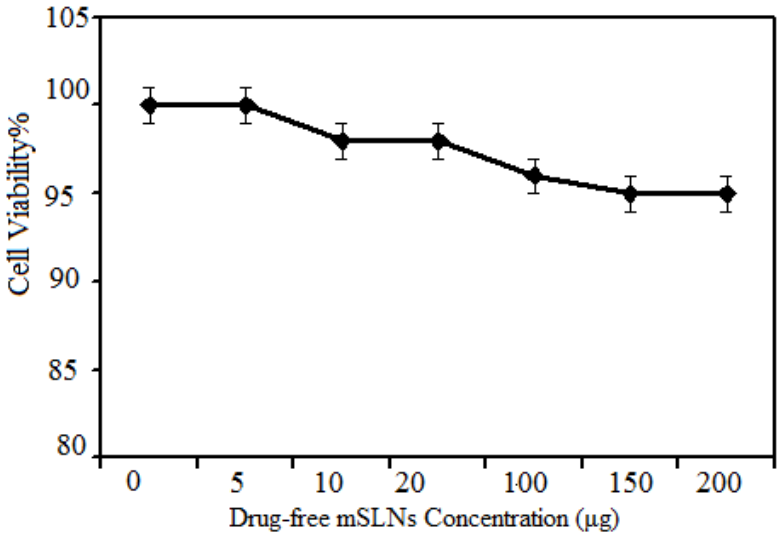

Fig. 5. The biocompatibility of the free drug-mSLNs on MCF-7 cells at various concentrations

in controlling drug release when temperatures rise. A PTX-loaded mSLN, they found, is a promising system for improving drug bioavailability, potentially improving cancer treatment in the future [31].

Based on a similar approach, Abidi et al. found that albendazole was gradually released from mSLNs after 36 hours, attaining a maximum of 84% after 48 hours. As a result of their research, they found that mSLNs are fast and highly efficient delivery systems for drugs [32].

An ultrasonic-solvent mixture method was developed by Ahmadifard and colleagues to prepare chitosan-coated mSLNs with letrozole. After applying a low-frequency pulsed magnetic field (LFPME) at 50Hz for 1 hour, this system achieved a 90.1% drug encapsulation rate, with 50% of the drug released, compared to the same amount of drug released over 12 hours using the non-LFPME application. Through the release of LTZ from a nano delivery system, as has been demonstrated in previous studies, they were able to control chemotherapy treatment in drug-resistant cancers through localized temperature induction through magnetic fields [33].

According to Ghiani et al., lipid nanoparticles synthesized with gadolinium (III) complexes were approximately 50 nm in size. PSLNs (paramagnetic solid lipid nanoparticles) developed in this study showed good stability. MRI studies were conducted using BALB/c nu/nu mice bearing IGROV-1 ovarian carcinomas. By administering folate intravenously, a targeting ligand, the nanoparticle surface was functionalized, enhancing the T1 signal in the tumor region. Observations of pSLN distribution in the liver of C57BL/6 mice suggested that hepatic clearance rates need to be improved through biodistribution adjustments [34].

A recent investigation by Rocha et al. outlined the creation of a new hybrid magnetic nanocomposite (mHNCs-DOX) that features a chemotherapeutic agent (DOX), superparamagnetic iron oxide nanoparticles (Fe3O4) serving as a T2 contrast medium, and paramagnetic manganese oxide nanoparticles (MnO) utilized as a T1-MRI contrast medium [35]. In vitro studies demonstrated that Hs578t cancer cells undergo simultaneous T1/T2 MRI and thermo-chemotherapy [35].

Compared to SLNs, mSLNs show better thermo-responsiveness [33,35], are efficient at targeting tumors [37], and are offered excellent biocompatibility [35,36]. Additionally, these nanosystems can be used to provide thermal therapy, as well as controlled drug release, with magnetic hyperthermia [32], Additionally, they can be used as contrast agents in MRIs [35].

There is widespread recognition that mSLNs and lipids are safe and compatible with biological systems. Our study confirmed the biocompatibility of mSLNs with drug-free components by evaluating their effects on MCF-7 cells at varying concentrations. The MCF-7 cells were tested with drug-free mSLNs ranging from 0.5 to 200 µg/mL, showing that their relative cytotoxicity remained

below 10% up to 0.6 mg/mL (Fig. 5). Therefore, the observed cytotoxicity associated with mSLNs can be attributed to the effects of EPI rather than the compositions of the nanocomplexes, given that the tested concentrations align with those used in the MTT assay. The toxicity observed was not due to the nanocomplex compositions, but rather the drug effects. These findings demonstrate the biocompatibility of the materials used to create the nanocomplexes, as well as the efficacy of carriers for intravenous drug delivery.

CONCLUSION

In the experiments, EPI was effectively encapsulated in magnetic solid lipid nanoparticles (SLN NPs) with a particle size appropriate for intravenous injection. The entrapment efficiencies achieved were 86±4.5% for SLNs and 51.7±3.5% for mSLNs. Particle size characterization indicated that the loaded magnetic nanoparticles led to an increase in the size of the prepared mSLNs. The nanometric particle size was proved by SEM micrographs of the samples. The data of release exponent "n" according to Korsmeyer–Peppas is also calculated and the value of 0.65 and 0.57 obtained for mSLNs and SLNs respectively. The obtained results showed by a combination of SLNs as an alternative drug carrier and magnetic nanoparticles the targeted drug delivery system could be prepared by increased in the drug release neither also in a controlled manner nor for burst form with superparamagnetic behavior. The cytotoxicity of optimized mSLNs in different cell lines proved the more cytotoxicity of mSLNs toward the MCF-7 cell line. In summary, the developed targeted drug delivery system demonstrates significant potential as a viable option for targeting and treating cancer, based on in vitro assessments.

CONFLICT OF INTEREST

The authors declare no conflict of interest.

ACKNOWLEDGEMENT

The authors gratefully acknowledge financial support (Grant No.: SCU.SC98.31316) from the Shahid Chamran University of Ahvaz. We thankful of Shohda Lab for cytotoxicity data.

REFERENCES

1. Gottesman, M.M., O. Lavi, M.D. Hall and J.-P. Gillet, Toward a better understanding of the complexity of cancer drug resistance. Annual review of pharmacology and toxicology, 2016. 56: p. 85-102. https://doi.org/10.1146/annurev-pharmtox-010715-103111
2. Wong, H.L., R. Bendayan, A.M. Rauth, Y. Li and X.Y. Wu, Chemotherapy with anticancer drugs encapsulated in solid lipid nanoparticles. Advanced drug delivery reviews, 2007. 59(6): p. 491-504. https://doi.org/10.1016/j.addr.2007.04.008
3. Ying, X.-Y., D. Cui, L. Yu and Y.-Z. Du, Solid lipid nanoparticles modified with chitosan oligosaccharides for the controlled release of doxorubicin. Carbohydrate Polymers, 2011. 84(4): p. 1357-1364. https://doi.org/10.1016/j.carbpol.2011.01.037
4. Rostami, E., Recent achievements in sodium alginatebased nanoparticles for targeted drug delivery, Polymer Bulletin, 2022. 79(2): p. 6885-6904. https://doi.org/10.1007/s00289-021-03781-z
5. Rostami, E., S. Kashanian and A. Azandaryani, Preparation of solid lipid nanoparticles as drug carriers for levothyroxine sodium with in vitro drug delivery kinetic characterization. Molecular biology reports, 2014. 41(5): p. 3521-3527. https://doi.org/10.1007/s11033-014-3216-4
6. Gasco, M.R., A. Mauro and G.P. Zara, 13 In Vivo Evaluations of Solid Lipid Nanoparticles and Microemulsions. Drug Delivery Nanoparticles Formulation and Characterization, 2016. 191: p. 219.
7. Martins, S.M., B. Sarmento, C. Nunes, M. Lúcio, S. Reis and D.C. Ferreira, Brain targeting effect of camptothecin-loaded solid lipid nanoparticles in rat after intravenous administration. European Journal of Pharmaceutics and Biopharmaceutics, 2013. 85(3): p. 488-502. https://doi.org/10.1016/j.ejpb.2013.08.011
8. Rostami, E. Progresses in targeted drug delivery systems using chitosan nanoparticles in cancer therapy: A mini-review, Journal of Drug Delivery Science and Technology, 2020 (58): p.101813. https://doi.org/10.1016/j.jddst.2020.101813
9. Yang, S.C., L.F. Lu, Y. Cai, J.B. Zhu, B.W. Liang and C.Z. Yang, Body distribution in mice of intravenously injected camptothecin solid lipid nanoparticles and targeting effect on brain. Journal of controlled release, 1999. 59(3): p. 299-307. https://doi.org/10.1016/S0168-3659(99)00007-3
10. Arduino, I., N. Depalo, F. Re, R. Dal Magro, A. Panniello, N. Margiotta, E. Fanizza, A. Lopalco, V. Laquintana and A. Cutrignelli, PEGylated solid lipid nanoparticles for brain delivery of lipophilic kiteplatin Pt (IV) prodrugs: An in vitro study. International journal of pharmaceutics, 2020. 583: p. 119351. https://doi.org/10.1016/j.ijpharm.2020.119351
11. Zhu, L., Z. Zhou, H. Mao and L. Yang, Magnetic nanoparticles for precision oncology: theranostic magnetic iron oxide nanoparticles for image-guided and targeted cancer therapy. Nanomedicine, 2016(0). https://doi.org/10.2217/nnm-2016-0316
12. Berry, C.C., Progress in functionalization of magnetic nanoparticles for applications in biomedicine. Journal of physics D: Applied physics, 2009. 42(22): p. 224003. https://doi.org/10.1088/0022-3727/42/22/224003
13. Wang, W., Y. Jing, S. He, J.-P. Wang and J.-P. Zhai, Surface modification and bioconjugation of FeCo magnetic nanoparticles with proteins. Colloids and Surfaces B: Biointerfaces, 2014. 117: p. 449-456. https://doi.org/10.1016/j.colsurfb.2013.11.050
14. Zhang, X., L. Xue, J. Wang, Q. Liu, J. Liu, Z. Gao and W. Yang, Effects of surface modification on the properties of magnetic nanoparticles/PLA composite drug carriers and

in vitro controlled release study. Colloids and Surfaces A: Physicochemical and Engineering Aspects, 2013. 431: p. 80-86. https://doi.org/10.1016/j.colsurfa.2013.04.021
15. Chomoucka, J., J. Drbohlavova, D. Huska, V. Adam, R. Kizek and J. Hubalek, Magnetic nanoparticles and targeted drug delivering. Pharmacological Research, 2010. 62(2): p. 144-149. https://doi.org/10.1016/j.phrs.2010.01.014
16. Wu, W., Z. Wu, T. Yu, C. Jiang and W.-S. Kim, Recent progress on magnetic iron oxide nanoparticles: synthesis, surface functional strategies and biomedical applications. Science and Technology of Advanced Materials, 2016. https://doi.org/10.1088/1468-6996/16/2/023501
17. Matuszak, J., J. Baumgartner, J. Zaloga, M. Juenet, A.E. Da Silva, D. Franke, G. Almer, I. Texier, D. Faivre and J.M. Metselaar, Nanoparticles for intravascular applications: physicochemical characterization and cytotoxicity testing. Nanomedicine, 2016. 11(6): p. 597-616. https://doi.org/10.2217/nnm.15.216
18. Oumzil, K., M.A. Ramin, C. Lorenzato, A. Hémadou, J. Laroche, M.J. Jacobin-Valat, S. Mornet, C.-E. Roy, T. Kauss and K. Gaudin, Solid Lipid Nanoparticles for imageguided therapy of atherosclerosis. Bioconjugate chemistry, 2016. 27(3): p. 569-575. https://doi.org/10.1021/acs.bioconjchem.5b00590
19. Zhao, S., Y. Zhang, Y. Han, J. Wang and J. Yang, Preparation and Characterization of cisplatin magnetic solid lipid nanoparticles (MSLNs): effects of loading procedures of Fe3O4 nanoparticles. Pharmaceutical research, 2015. 32(2): p. 482-491. https://doi.org/10.1007/s11095-014-1476-2
20. Lodhia, J., G. Mandarano, N. Ferris, P. Eu and S. Cowell, Development and use of iron oxide nanoparticles (Part 1): Synthesis of iron oxide nanoparticles for MRI. Biomed Imaging Interv J, 2010. 6(2): p. e12. https://doi.org/10.2349/biij.6.2.e12
21. Afshari, M., K. Derakhshandeh and L. Hosseinzadeh, Characterisation, cytotoxicity and apoptosis studies of methotrexate-loaded PLGA and PLGA-PEG nanoparticles. Journal of microencapsulation, 2014. 31(3): p. 239-245. https://doi.org/10.3109/02652048.2013.834991
22. Derakhshandeh, K., M. Soheili, S. Dadashzadeh and R. Saghiri, Preparation and in vitro characterization of 9-nitrocamptothecin-loaded long circulating nanoparticles for delivery in cancer patients. Int J Nanomedicine, 2010. 5(1): p. 1-9. https://doi.org/10.2147/IJN.S11586
23. Sahoo, J., P. Murthy and S. Biswal, Formulation of sustained-release dosage form of verapamil hydrochloride by solid dispersion technique using Eudragit RLPO or kollidon® SR. AAPS PharmSciTech, 2009. 10(1): p. 27-33. https://doi.org/10.1208/s12249-008-9175-0
24. Lokhandwala, H., A. Deshpande and S. Deshpande, Kinetic modeling and dissolution profiles comparison: an overview. Int. J. Pharm. Bio. Sci, 2013. 4(1): p. 728-73.
25. Ding, J., Chen, G., ,Guofang Chen, G., and Gu, M. One-Pot Synthesis of Epirubicin-Capped Silver Nanoparticles and Their Anticancer Activity against Hep G2 Cells, Pharmaceutics. 2019. 11(3): p.123 https://doi.org/10.3390/pharmaceutics11030123
26. Mikhaylova, M., D.K. Kim, N. Bobrysheva, M. Osmolowsky, V. Semenov, T. Tsakalakos and M. Muhammed, Superparamagnetism of magnetite nanoparticles: dependence on surface modification. Langmuir, 2004. 20(6): p. 2472-2477. https://doi.org/10.1021/la035648e
27. Chen, H., L.Q. Xie, J. Qin, Y. Jia, X. Cai, W. Nan, W. Yang, F. Lv and Q.Q. Zhang, Surface modification of PLGA nanoparticles with biotinylated chitosan for the sustained in vitro release and the enhanced cytotoxicity of epirubicin. Colloids and Surfaces B: Biointerfaces, 2016. 138: p. 1-9. https://doi.org/10.1016/j.colsurfb.2015.11.033
28. Markides, H., M. Rotherham and A. El Haj, Biocompatibility and toxicity of magnetic nanoparticles in regenerative medicine. Journal of Nanomaterials, 2012. 2012. https://doi.org/10.1155/2012/614094
29. Jain, T.K., M.K. Reddy, M.A. Morales, D.L. Leslie-Pelecky and V. Labhasetwar, Biodistribution, clearance, and biocompatibility of iron oxide magnetic nanoparticles in rats. Molecular pharmaceutics, 2008. 5(2): p. 316-327. https://doi.org/10.1021/mp7001285
30. Pang, X., Cui, F., Tian, J., Chen, J., Zhou, J., Zhou, W. Preparation and characterization of magnetic solid lipid nanoparticles loaded with ibuprofen. Asian Journal of Pharmaceutical Science, 2009, 4, p.132-137.
31. Oliveira, R.R., Carrião, M., Pacheco, M.T., Branquinho, L.C., de Souza, A.L.R., Bakuzis, A., Lima, E.M. Triggered release of paclitaxel from magnetic solid lipid nanoparticles by magnetic hyperthermia. Materials Science and Engineering: A , 2018, 92, p.547-553. https://doi.org/10.1016/j.msec.2018.07.011
32. Abidi, H., Ghaedi, M., Rafiei, A., Jelowdar, A., Salimi, A., Asfaram, A., Ostovan, A. Magnetic solid lipid nanoparticles co-loaded with albendazole as an anti-parasitic drug: Sonochemical preparation, characterization, and in vitro drug release. Journal of Molecular Liquid, 2018, 268, p.11-18. https://doi.org/10.1016/j.molliq.2018.06.116
33. Ahmadifard, Z., Ahmeda, A., Rasekhian, M., Moradi, S., Arkan, E. Chitosan-coated magnetic solid lipid nanoparticles for controlled release of letrozole. Journal of Drug Delivery Science and Technology. 2020, 57, p.101621. https://doi.org/10.1016/j.jddst.2020.101621
34. Grillone, A., Battaglini, M., Moscato, S., Mattii, L., Fernández, C.D.J., Scarpellini, A., Giorgi, M., Sinibaldi, E., Ciofani, G. Nutlin-loaded magnetic solid lipid nanoparticles for targeted glioblastoma treatment. Nanomedicine 2019, 14, p. 727-752. https://doi.org/10.2217/nnm-2018-0436
35. Rocha, C.V., da Silva, M.C., Bañobre-López, M., Gallo, J. (Para) magnetic hybrid nanocomposites for dual MRI detection and treatment of solid tumours. Chemical Communication. 2020, 56, p. 8695-8698. https://doi.org/10.1039/D0CC03020A
36. Abakumov, M.A., Semkina, A.S., Skorikov, A.S., Vishnevskiy, D.A., Ivanova, A.V., Mironova, E., Davydova, G.A., Majouga, A.G., Chekhonin, V.P. Toxicity of iron oxide nanoparticles: Size and coating effects. Journal of Biochemistry Molecular Toxicology. 2018, 32, p.e22225. https://doi.org/10.1002/jbt.22225
37. Hsu, M.-H., Su, Y.-C. Iron-oxide embedded solid lipid nanoparticles for magnetically controlled heating and drug delivery. biomedical microdevices journal, 2008, 10, p.785-793. https://doi.org/10.1007/s10544-008-9192-5